

Precursor effects and premartensitic transformation in Ni₂MnGa

A. Zheludev, S. M. Shapiro, and P. Wochner
Brookhaven National Laboratory, Upton, New York 11973

L. E. Tanner
Lawrence Livermore National Laboratory, Livermore, California 94550
(Received 29 March 1996; revised manuscript received 12 August 1996)

Inelastic neutron scattering and neutron diffraction were used to study a single crystal of the Ni₂MnGa shape memory Heusler alloy in a wide temperature range covering the parent phase ($T > T_1 = 260$ K), a premartensitic phase ($T_1 > T > T_M$), and a martensitic ($T < T_M = 220$ K) phase region. Several anomalies in the phonon dispersion curves in the parent phase were observed. The premartensitic phase involves a transverse modulation of the parent cubic structure with a simple periodicity of $(\frac{1}{3}, \frac{1}{3}, 0)$. The approximately tetragonal lattice of the low-temperature martensite is distorted by transverse modulations with incommensurate wave vectors $(\zeta_M, \zeta_M, 0)$, $\zeta_M \approx 0.43$. The observed phenomena are attributed to electron-phonon interactions and anharmonic effects. [S0163-1829(96)07345-6]

I. INTRODUCTION

Martensitic phase transformations (MT's) are defined as displacive, diffusionless first-order transitions from a symmetric high-temperature phase to a low-symmetry product martensitic structure at low temperature.¹ MT's have been extensively studied for over a century because of the importance of the product phase in metallurgy and the key role played by MT in the shape memory phenomenon. In recent years much attention has been given to precursor effects where acoustic anomalies, phonon dispersion curves, and diffuse elastic scattering in the parent phase give an indication of the eventual martensitic structure. For example, in a number of bcc materials the $(\zeta, \zeta, 0)$ TA₂ mode with displacement along $(1\bar{1}0)$ softens at a certain wave vector ζ_0 which is close to a reciprocal-lattice vector of the low-temperature structure. This has been demonstrated in extensive studies of Ni-Ti (Refs. 2–5), Ni-Al (Refs. 6–9 and references therein), Au-Cd (Ref. 10), and other bcc-based alloys.

One interesting model system for studying MT is the Ni₂MnGa Heusler alloy, a material which combines bulk ferromagnetism ($T_C \approx 380$ K) with shape-memory behavior and a MT at $T_M \approx 220$ K (Ref. 11). A number of thermal and stress-induced martensitic structures have been observed in this compound¹² and were investigated by x-ray diffraction,^{11,12} electron diffraction and microscopy,^{11,13} ultrasound experiments,^{14,13,15} and magnetoelastic measurements.^{14,16} Recently we have carried out an inelastic neutron scattering investigation of the martensitic precursor phenomena in Ni₂MnGa.¹⁷ A significant, nearly complete, softening of the $(\zeta_0, \zeta_0, 0)$, $\zeta_0 \approx \frac{1}{3}$ transverse acoustic phonon with polarization along (110) , suggested by Fritsch *et al.*,¹⁸ has been observed in the parent phase as $T \rightarrow T_M$. A new premartensitic (PM) phase transition was observed at $T_1 \approx 260$ K, although its relation to the low-temperature martensitic transition was not fully understood.

In the present paper we report the results of further neu-

tron diffraction and inelastic scattering experiments. Our goals were to search for additional phonon anomalies in the high-temperature phase, investigate the structure and lattice dynamics in the PM phase, and study the low-temperature martensite. The data obtained allow us to discuss the dynamics of the two-step phase transformation in Ni₂MnGa. Preliminary results of this work were reported elsewhere.¹⁹

II. EXPERIMENT

At room temperature Ni₂MnGa has a fcc $L2_1$ Heusler structure (space group $Fm\bar{3}m$, No. 225), the cell constant being 5.822 Å (Ref. 11). If the Mn and Ga sites are not distinguished, the structure can be viewed as being composed of eight CsCl-type units ($a_{\text{CsCl}} = \frac{1}{2}a_{\text{fcc}}$), with Ni at the cube center and Mn and Ga at the corners. Three types of Bragg reflections exist: the order-independent principal bcc reflections with $h+k+l=4n$ (structure factor $F=4(2b_{\text{Ni}}+b_{\text{Mn}}+b_{\text{Ga}}) \approx 9.66 \times 10^{-12}$ cm), reflections of type $h+k+l=4n+2$ [$F=4(2b_{\text{Ni}}-b_{\text{Mn}}-b_{\text{Ga}}) \approx 6.82 \times 10^{-12}$ cm] corresponding to a $B2$ (CsCl-type) structure, and the fcc superlattice reflections with h, k, l all odd [$F=4(b_{\text{Mn}}-b_{\text{Ga}}) \approx -4.41 \times 10^{-12}$ cm]. The use of $B2$ indexing may be sometimes found in the literature, but for the sake of clarity the correct fcc notation will be used throughout this paper.

We have made use of the same single-crystal sample as in our previous studies.¹⁷ It was grown by the Bridgman method at Ames Laboratory particularly for these experiments. The 7-cm-long sample had the shape of a half cylinder, 1.5 cm in diameter. The longer dimension was identified as (111) . The martensitic phase transition temperature $T_M \approx 220$ K was estimated from the splitting of the (220) Bragg peak which occurs at 212 K on cooling and 228 K on warming up [Fig. 1(a)], thus showing a significant temperature hysteresis. The MT was found to be completely reversible. As will be discussed in detail below, the low-temperature martensitic structure is roughly tetragonal with a complex incommensurate (110) -transverse modulation.

Neutron scattering experiments were carried out on the

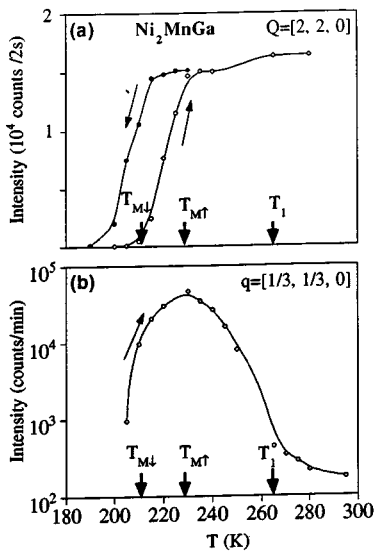


FIG. 1. (a) Elastic intensity measured in the (220) Bragg position as a function of temperature. The disappearance of the Bragg peak at low temperature indicates the martensitic transformation. $T_{M\uparrow}$ and $T_{M\downarrow}$ indicate the temperatures at which the martensitic phase disappears on warming up and first appears on cooling. (b) Temperature dependence of the intensity in the $(\frac{1}{3}, \frac{1}{3}, 0)$ elastic satellite in cubic Ni_2MnGa . The peak is characteristic of the pre-martensitic phase.

H4M and H8 triple-axis spectrometers at the HFBR at Brookhaven National Laboratory. The use of standard and high-temperature Displex refrigerators enabled us to perform the measurements over a wide temperature range 12–400 K. Two sample settings were used. The crystal was aligned to have either the (100) or the (110) planes coincide with the scattering plane of the spectrometer. The sample mosaic reveals two monocrystalline grains, misaligned by 0.5° , giving a full width at half maximum (FWHM) of 1° . Neutron scattering experiments were performed with fixed final or initial

neutron energies, $E = 14.7$ meV and $E = 30.5$ meV. Pyrolytic graphite PG(002) reflections were used for monochromator and analyzer. $20' - 20' - 20' - 40'$ and $40' - 20' - 20' - 40'$ collimations were used, yielding a typical energy resolution of $\delta E = 0.4$ meV and $\delta E = 0.7$ meV full width at half maximum at $\Delta E = 0$, $E_f = 14.7$ meV, and 30.5 meV, respectively. A pyrolytic graphite filter was positioned in front of the detector or in front of the sample for E_f -constant and E_i -constant measurements, respectively. Both constant- q and constant- E scans were utilized to determine the phonon cross section.

III. RESULTS

A. Precursor phenomena in the parent phase

1. Phonon dispersion

Phonon dispersion curves¹⁹ were determined from inelastic neutron scattering along the high-symmetry directions $(\zeta, 0, 0)$, $(\zeta, \zeta, 0)$, (ζ, ζ, ζ) , and $(2\zeta, \zeta, \zeta)$. The results are shown in Fig. 2. The curves are plotted in an extended Brillouin zone scheme of the fcc $L2_1$ structure, that is, in the reduced zone scheme for the $B2$ structure.

Most modes demonstrate only slight temperature dependence easily explained by the overall stiffening of the lattice at low temperatures. The most striking feature, however, is the strong temperature dependence of the $(\zeta, \zeta, 0)$ TA_2 branch with polarization along (110), discussed in detail in our previous paper.¹⁷ As shown in the blowup in Fig. 3(a) (dashed lines), the dispersion curve has a wiggle at $\zeta_0 \approx \frac{1}{3}$ at room temperature, which develops into a distinct minimum as the temperature is decreased. In the limit $\zeta \rightarrow 0$ the $(\zeta, \zeta, 0)$ TA_2 mode corresponds to the elastic constant $c' = \frac{1}{2}(c_{11} - c_{12})$, which is known to be reduced in bcc materials,²⁰ and shows an anomalous decrease as $T \rightarrow T_M$ in Ni_2MnGa (Refs. 14 and 13). For the (110) direction, the slopes in the longitudinal ($v_L \approx 5.4 \times 10^5$ cm/s) and (001) transverse ($v_{T1} \approx 3.5 \times 10^5$ cm/s) dispersion curves at $q \rightarrow 0$ are in good agreement with experimental ultrasound

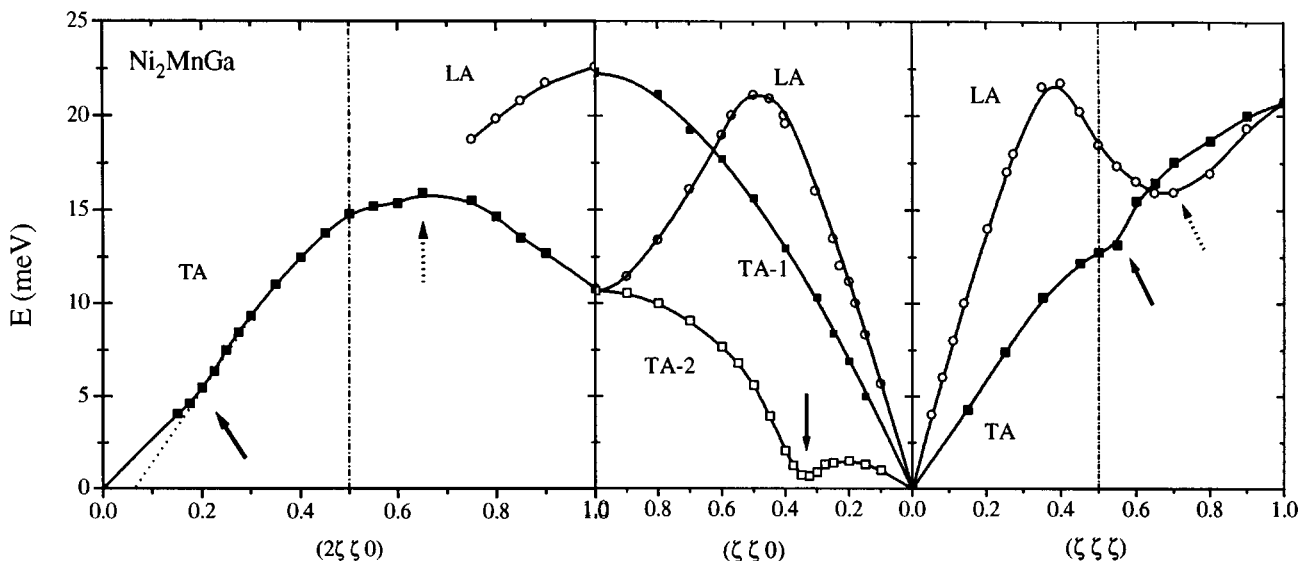


FIG. 2. Measured acoustic-phonon dispersion curves for the parent $L2_1$ phase of Ni_2MnGa ; the dash-dotted lines show the fcc zone boundaries. Solid lines are guides to the eye and arrows indicate the observed phonon anomalies.

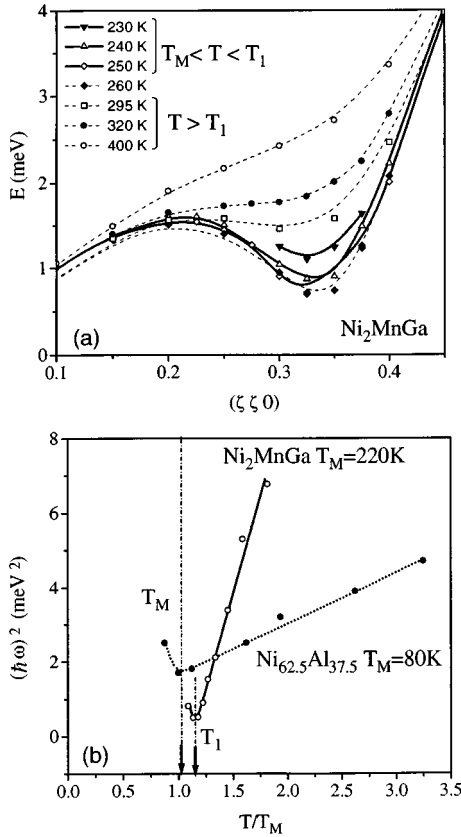


FIG. 3. (a) Temperature dependence of the phonon anomaly in the $(\zeta, \zeta, 0)$ TA_2 branch in the parent (dashed lines) and the PM (solid lines) phases of Ni_2MnGa . (b) $(\hbar\omega)^2$ vs T/T_M for the $(\zeta, \zeta, 0)$ TA_2 mode for Ni_2MnGa and $Ni_{62.5}Al_{37.5}$ in the point where the dispersion curve is a minimum. The Ni-Al data are taken from S. M. Shapiro *et al.* [Phys. Rev. B **26**, 9301 (1991)].

velocities.^{14,13,15} In contrast, a significant discrepancy is found for the $(1\bar{1}0)$ -transverse sound velocity which is estimated to be $v_{T2} \approx 1.0 \times 10^5$ cm/s from our neutron data and $v_{T2} \approx 4.1 \times 10^5$ cm/s from ultrasound experiments performed by Vasil'ev *et al.*¹⁴ More recent ultrasound data obtained Triosonno¹⁵ on a samples cut from the single crystal used in our neutron experiments are in perfect agreement with neutron scattering results.

Figure 4(a) shows a plot of the phonon energy measured in a perpendicular (110) direction from the $\mathbf{q} = (\frac{1}{3}, \frac{1}{3}, 0)$ reciprocal space point, where the phonon energy is a minimum. The solid line in Fig. 4(a) represents a least-squares fit with the empirical “gap” relation $(\hbar\omega)^2 = \Delta^2 + c^2 q_{\perp}^2$ where Δ is the temperature-dependent gap at $\mathbf{q} = (\frac{1}{3}, \frac{1}{3}, 0)$, c is the appropriate sound velocity, and q_{\perp} is the wave vector along (110) , relative to $\mathbf{q} = (\frac{1}{3}, \frac{1}{3}, 0)$. $(\hbar\omega)$ increases dramatically, as the wave vector deviates from the (110) direction. Thus the anomaly in the dispersion manifold is restricted to a narrow valley along (110) . This behavior is similar to that of the corresponding mode in Ni-Al alloys,⁶ though phonon softening is much more pronounced in Ni_2MnGa . Figure 3(b) compares the temperature dependence of the TA_2 soft-mode frequencies in Ni_2MnGa and $Ni_{62.5}Al_{37.5}$ (Ref. 6). $(\hbar\omega)^2$ decreases linearly with temperature in both materials. Note that it extrapolates to zero at $T_0 = 250$ K $> T_M \approx 220$ K

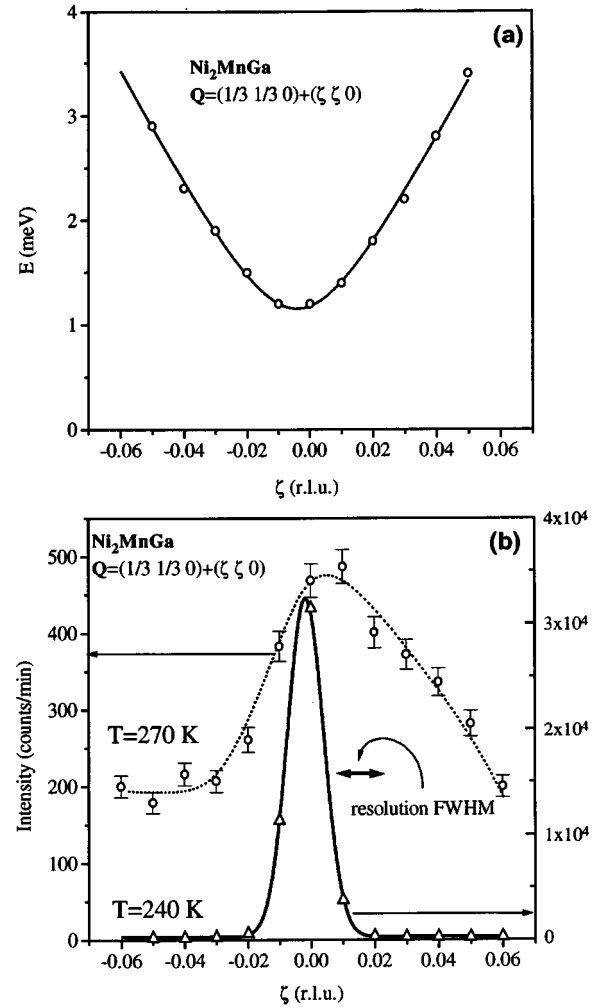


FIG. 4. (a) Phonon energies measured along $\mathbf{q} = (\frac{1}{3}, \frac{1}{3}, 0) + (\zeta, -\zeta, 0)$ in the parent phase. (b) Elastic scans in the same direction: Diffuse scattering in the parent phase (dotted line) is replaced by a sharp Bragg-like peak in the PM phase (solid line).

and $T_0 = -35$ K $\ll T_M \approx 80$ K in Ni_2MnGa and $Ni_{62.5}Al_{37.5}$, respectively. As will be discussed below, the upturn at low temperatures indicates the formation of a new phase below $T_1 \approx 260$ K in Ni_2MnGa and the martensitic phase below T_M in the Ni-Al alloy.

As indicated by solid arrows in Fig. 2, the (ζ, ζ, ζ) and possibly the $(2\zeta, \zeta, 0)$ TA branches show slight “wiggles” at finite wave vectors. Similar features were predicted and later observed experimentally in Ni-Al alloys.⁹ These anomalies, together with the dip in the $(\zeta, \zeta, 0)$ TA_2 mode, are probably due to e -ph coupling and nesting features of the Fermi surface.

Another prominent feature (dotted arrows in Fig. 2) is the dip in the (ζ, ζ, ζ) LA branch at $\mathbf{q} = (\frac{2}{3}, \frac{2}{3}, \frac{2}{3})$. It corresponds to a broad plateau in the $(2\zeta, \zeta, \zeta)$ dispersion curve at the equivalent wave vector $\mathbf{q} = (\frac{4}{3}, \frac{2}{3}, \frac{2}{3})$. Present in all bcc metals, this anomaly is the signature of the Coulomb contribution of positive ions in a bcc arrangement to the dynamical matrix. It may in some cases be enhanced by e -ph interaction^{21,22} and is relevant to the formation of the so-called ω phase.^{23–25} Apparently, it is not related to the MT in Ni_2MnGa , since no temperature dependence was observed.

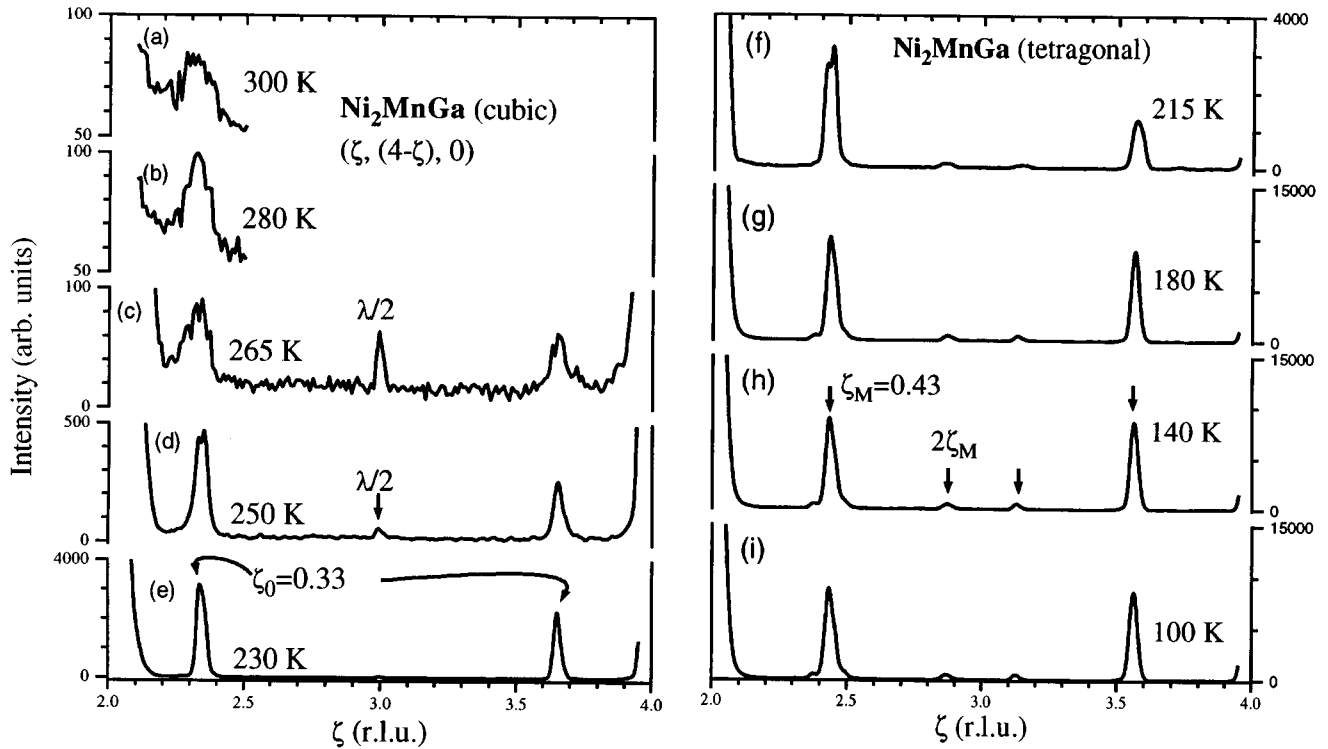


FIG. 5. Elastic scattering in the $(\zeta, \zeta, 0)$ direction measured at different temperatures. The diffuse central peak in the parent phase (a)–(c) transforms into a Bragg-like satellite characteristic of the PM phase at lower temperatures (d) and (e). Transverse elastic scans along $(\zeta, \zeta, 0)$ in the martensitic phase reveal a different incommensurate superstructure (f)–(i).

2. Quasielastic scattering for $T > T_1$

As has been previously reported,¹⁷ there is diffuse quasielastic scattering associated with the overall low energy of the $(\zeta, \zeta, 0)$ TA_2 phonon dispersion [Figs. 5(a)–5(c)]. This elastic intensity is a combination of two effects: The first is diffuse scattering which diverges as $\zeta \rightarrow 0$ [viz., Huang diffuse scattering (HDS)]; the second is a satellite peak at ζ_0 , the “central peak,”¹⁷ associated with the dip in the TA_2 dispersion manifold. The shape of the satellite in q space [Fig. 4(b), dashed line] roughly coincides with the inverse the dip in the dispersion manifold and its q width is T independent ($\Delta q \approx 0.15 \text{ \AA}^{-1}$) at $T > T_1$. The energy width of the peak is resolution limited. Figure 4(b) shows that, just as the phonon anomaly, it is localized in a narrow valley along (110) . As argued in Ref. 17 the diffuse peak is defect, induced and is directly related to the reduction of vibrational frequencies as explained by the model proposed by Axe *et al.*²⁶ and Halperin and Varma.²⁷

B. “Premartensitic” transition

The progressive softening of TA_2 phonons propagating in the (110) direction leads to a PM phase transition at $T_1 \approx 260 \text{ K}$. The first indication to the existence of this phase was obtained in magnetoelastic measurements.¹⁶ Though the PM transition, unlike the MT at a lower temperature, does not manifest itself in the magnetic susceptibility curves,¹¹ magnetostriction shows a distinct kink at T_1 .

The best evidence for the existence of the PM phase is the behavior of the $(\zeta_0, \zeta_0, 0)$, $\zeta_0 = \frac{1}{3}$ elastic satellite [displacements along (110)]. At higher temperatures the peak is

broad and relatively weak [Figs. 5(a)–5(c)]. As the temperature decreases below T_1 it becomes narrow and Bragglike [Fig. 5(d)–5(e)]. Its intensity increases dramatically and its q width becomes defined by the experimental resolution, rather than the shape of the dip in the phonon dispersion curve. The same may be seen from elastic scans along the $(1\bar{1}0)$ direction from the $(\frac{1}{3}, -\frac{1}{3}, 0)$ point. Again, the peak appears much narrower than the phonon anomaly, and is resolution limited in this direction.

It could be expected that the formation of the PM phase, which is characterized by a new $(\frac{1}{3}, \frac{1}{3}, 0)$ transverse modulation of the parent cubic structure, should be accompanied by a uniform distortion of the latter. Experimentally, this has not been observed: Neither splitting nor shifting of the original fcc Bragg peaks was detected below T_1 . Only their intensity decreases slightly below T_1 , as could have been expected, considering the formation of new superlattice Bragg peaks.

A characteristic of the PM phase is the *stiffening* of the $(\zeta_0, \zeta_0, 0)$ TA_2 phonon with decreasing temperature. This is borne out in Fig. 3. The fact that the phonon softening is *incomplete* suggests that the phase transformation in Ni_2MnGa at T_1 is of the first order and is not a Cochran-Anderson complete soft-mode transition of the type seen in materials like $SrTiO_3$.²⁸

C. Low-temperature martensite

Cooling the PM phase through T_M produces a conventional martensitic transformation, which, like the Ni-Al system, involves *both* a periodic modulation and a strong tetragonal distortion of the lattice. Relying on the results of x-ray

diffraction experiments, Martynov and Kokorin¹² suggested that the martensitic phase is approximately tetragonal with $a=b=5.90$ Å, $c=5.54$ Å, and $c/a=0.94$, modulated along $(\zeta_M, \zeta_M, 0)$, $\zeta_M=0.4$ with displacements along (110) [five-layer (220) plane martensite]. This implies that in a transverse elastic scan from $(220)_{\text{tet}}$ to $(400)_{\text{tet}}$ four equally spaced superstructure Bragg peaks should appear. Our experiments [Figs. 5(f)–5(i)] show that the actual situation is different. Indeed, four peaks are observed, but they are *not* equally spaced. Their positions $(\pm \zeta_M, \pm \zeta_M, 0)_{\text{tet}}$ and $(\pm 2\zeta_M, \pm 2\zeta_M, 0)_{\text{tet}}$, $\zeta_M \approx 0.43$, found to be the same in several Brillouin zones, correspond to an incommensurate modulation of the average tetragonal structure along the $(110)_{\text{tet}}$ direction with displacements along $(1\bar{1}0)_{\text{tet}}$. Such a periodicity is *substantially different from the one in the PM phase*, where the modulation occurs with $\zeta \approx 0.33$. It is also important to emphasize that *no phonon anomalies were observed above T_M at $\zeta \approx 0.43 = \zeta_M$* .

IV. DISCUSSION

The diffusionless phase transitions in Ni_2MnGa may be adequately described by a Landau-type phenomenological free energy functional \mathcal{F} (Ref. 29). The theory should be able to account for (1) a first-order phase transition at T_1 with incomplete phonon softening, resulting in a periodic distortion of the cubic phase with the wave vector of the soft mode, (2) the MT at T_M which involves both a tetragonal distortion and a new superstructure, and (3) the fact that the superstructure in the MT phase has a different periodicity from that of the “softest” $(\zeta_0, \zeta_0, 0)$ phonon and is incommensurate with the tetragonal lattice. For this, the theory should make use of a suitable set of order parameters, including the tensor of uniform strains $e_{\mu\nu}$ and the amplitudes of periodic $(\zeta, \zeta, 0)$ distortions of the parent structure $\eta(\zeta)$ (Refs. 30–33). Requirement (1) may be met by appropriately choosing the signs of higher-order Landau coefficients when expanding \mathcal{F} to a series in $\eta(\zeta_0)$ (Ref. 30). As the temperature is decreased, a global minimum in \mathcal{F} may appear at $\eta(\zeta_0) \neq 0$, before the $\eta(\zeta_0) = 0$ point (the parent phase) becomes dynamically unstable, i.e., before the phonon frequency reaches zero. This results in a “premature” first-order phase transition at $T_1 > T_0$. To meet requirement (2) one has to consider anharmonic terms, coupling the order parameters η and $e_{\mu\nu}$ (Refs. 31–33). These are expected to be strong, since the application of uniaxial strain leads to a whole series of MT in Ni_2MnGa .¹² Requirement (3) requires strong wave vector dependence of the Landau coefficients. The free energy should be minimized with respect to $\eta(\zeta)$ for all plausible wave numbers ζ , and not only for ζ_0 . As a result, as in the case for Ni-Al alloys, the modulation of the MT phase may correspond to wave vectors, different from that of the soft mode.^{31,6,34} The actual phase diagram is the result of a delicate competition between different anharmonic terms. The above description covers the cases of complete phonon softening ($T_0 = T_M$), as in SrTiO_3 (Ref. 28); one-step transitions with little phonon softening ($T_0 < T_M$), as in AuCuZn_2 , for example;³⁵ and the two-step transitions ($T_0 > T_M$) as in Ni_2MnGa and Ni-Ti (Refs. 3–5,36).

Naturally, phenomenological theories are able to explain neither the origin of the phonon anomalies nor their coupling

to uniform strains. Showing that the “wiggle” in the $(\zeta, \zeta, 0)$ TA_2 phonon dispersion curve in Ni_2MnGa persists above the ferromagnetic transition temperature¹⁷ ($T_C \approx 380$ K), we have ruled out the possibility of relating the dispersion anomalies to phonon-magnon interactions, a mechanism which is active in several magnetically ordered systems.^{37,38} Nevertheless, the phonon anomalies and phase transformation in Ni_2MnGa may be expected to be dependent on external magnetic fields, since both the MT and PM transition are accompanied by kinks in magnetostriction.¹⁶ It is generally agreed that the true origin of the phonon anomalies lies in electron-phonon (e -ph) coupling and specific nesting properties of the multiply connected Fermi surface.³⁹ The effect is similar to that produced by Kohn anomalies,⁴⁰ but stems from the divergence in the e -ph matrix element, rather than in the dielectric susceptibility itself. First-principles local-density-functional calculations,^{41,42} based on these concepts, were remarkably successful in reproducing the anomalies in the $(\zeta, \zeta, 0)$ TA_2 branches in Ni-Al and Ni-Ti alloys, and also predicted the weaker “wiggle” in the (ζ, ζ, ζ) TA mode, which was later observed experimentally.⁹ Both features are present in the phonon dispersion curves of Ni_2MnGa , suggesting that these systems have similar Fermi surfaces. It would be very interesting to see *ab initio* calculations for Ni_2MnGa . For the verification of the phenomenological and microscopic theories, much valuable information may be drawn from the study of the stress dependence^{7,8} of the phonon dispersion curves. We have recently performed such measurements on Ni_2MnGa and observed some very interesting uniaxial stress-dependent behavior.⁴³ In the future the investigation of the composition dependence⁶ may also prove extremely fruitful.

V. CONCLUSION

A system undergoing a two-step martensitic phase transformation was studied by inelastic neutron scattering and neutron diffraction. Several anomalies in the phonon dispersion curves were observed in the parent cubic phase. The nearly complete softening in the $(\zeta, \zeta, 0)$ TA_2 branch results in a premartensitic first-order phase transition which involves a commensurate periodic distortion of the parent structure with the periodicity equal to that of the soft mode. A strong wave vector dependence of the coupling of periodic distortions to homogeneous strains leads to a further transformation to an incommensurate martensitic phase at lower temperatures. The modulation of the martensite structure is distinct from that in the premartensitic phase.

ACKNOWLEDGMENTS

The authors would like to thank J. Trivisonno for interesting discussions and for sharing unpublished results. Work at Brookhaven National Laboratory was supported by the Division of Material Sciences, U.S. Department of Energy, under Contract No. DE-AC02-76CH00016. The work at Lawrence Livermore National Laboratory was performed under U.S. Department of Energy Contract No. W-7405-ENG-48.

- ¹Z. Nishiyama, *Martensitic Transformations* (Academic, New York, 1978).
- ²S. M. Shapiro, Y. Noda, Y. Fujii, and Y. Yamada, *Phys. Rev. B* **30**, 4314 (1984).
- ³S. K. Satija, S. M. Shapiro, M. B. Salamon, and C. M. Wayman, *Phys. Rev. B* **29**, 6031 (1984).
- ⁴P. Moine, J. Allain, and B. Renker, *J. Phys. F* **14**, 2517 (1984).
- ⁵H. Teitze, M. Muller, and B. Renker, *J. Phys. C* **17**, L529 (1984).
- ⁶S. M. Shapiro *et al.*, *Phys. Rev. B* **44**, 9301 (1991).
- ⁷S. M. Shapiro, E. C. Svensson, C. Vettier, and B. Hennion, *Phys. Rev. B* **48**, 13 223 (1993).
- ⁸L. Ye, S. M. Shapiro, and H. Chou, *Scr. Metall. Mater.* **31**, 203 (1994).
- ⁹H. Chou and S. M. Shapiro, *Phys. Rev. B* **48**, 16 088 (1993).
- ¹⁰T. Ohba, S. M. Shapiro, S. Aoki, and K. Otsuka, *Jpn. J. Appl. Phys.* **33**, L1631 (1994).
- ¹¹P. J. Webster, K. R. A. Ziebeck, S. L. Town, and M. S. Peak, *Philos. Mag.* **49**, 295 (1984).
- ¹²V. V. Martynov and V. V. Kokorin, *J. Phys. (France) III* **2**, 739 (1992).
- ¹³V. A. Chernenko and V. V. Kokorin, *Proceedings of the International Conference on Martensitic Transformations* (Monterey Institute for Advanced Studies, Monterey, CA, 1992), p. 1205.
- ¹⁴A. N. Vasil'ev, V. V. Kokorin, Y. I. Savchenko, and V. A. Chernenko, *Sov. Phys. JETP* **71**, 803 (1990).
- ¹⁵J. Trivisonno (unpublished).
- ¹⁶S. David, Master's thesis, CNRS, Laboratoire de Magétisme Louis Neel, Grenoble, 1991.
- ¹⁷A. Zheludev *et al.*, *Phys. Rev. B* **51**, 11 310 (1995).
- ¹⁸G. Fritsch, V. V. Kokorin, and A. Kempf, *J. Phys. Condens. Matter* **6**, L107 (1994).
- ¹⁹A. Zheludev *et al.*, *J. Phys. (Paris) III Colloq.* **5**, C8-1139 (1996).
- ²⁰C. Zener, *Phys. Rev.* **71**, 846 (1947).
- ²¹C. Stassis, J. Zarestky, and N. Wakabayashi, *Phys. Rev. Lett.* **41**, 1726 (1978).
- ²²W. Petry *et al.*, *Phys. Rev. Lett.* **61**, 722 (1988).
- ²³S. K. Sikka, Y. K. Vohra, and J. R. Chidambaram, *Prog. Mater. Sci.* **27**, 245 (1982).
- ²⁴H. E. Cook, *Phys. Rev. B* **15**, 1477 (1977).
- ²⁵D. de Fontaine, *Metall. Trans. A* **19**, 169 (1988).
- ²⁶J. D. Axe, S. M. Shapiro, G. Shirane, and T. Riste, in *Anharmonic Lattice, Structural Transitions and Melting*, edited by T. Riste (Nordhoff, Leiden, 1974).
- ²⁷B. I. Halperin and C. M. Varma, *Phys. Rev. B* **14**, 4030 (1976).
- ²⁸*Structural Phase Transitions*, edited by A. D. Bruce and R. A. Cowley (Taylor & Francis, London, 1981).
- ²⁹L. D. Landau and E. M. Lifshitz, *Statistical Physics I*, 3rd ed. (Pergamon, Oxford, 1980), Chap. 14.
- ³⁰J. A. Krumhansl and R. J. Gooding, *Phys. Rev. B* **39**, 3047 (1989).
- ³¹R. J. Gooding and J. A. Krumhansl, *Phys. Rev. B* **39**, 1535 (1989).
- ³²Y. Yamada, Y. Noda, and K. Fuchizaki, *Phys. Rev. B* **42**, 10 405 (1990).
- ³³J. A. Krumhansl, *Solid State Commun.* **84**, 251 (1992).
- ³⁴S. M. Shapiro *et al.*, *Phys. Rev. Lett.* **62**, 1298 (1989).
- ³⁵M. Mori, Y. Yamada, and G. Shirane, *Solid State Commun.* **17**, 127 (1975).
- ³⁶G. D. Sandrock, A. J. Perkins, and R. F. Heheman, *Metall. Trans.* **2**, 2769 (1971).
- ³⁷R. D. Lowde *et al.*, *Proc. R. Soc. London A* **374**, 87 (1981).
- ³⁸M. Sato, B. H. Grier, S. M. Shapiro, and H. Miyajima, *J. Phys. F* **12**, 2117 (1982).
- ³⁹C. M. Varma and W. Weber, *Phys. Rev. B* **19**, 6142 (1979).
- ⁴⁰R. N. Bhatt and W. L. McMillan, *Phys. Rev. B* **12**, 2042 (1975).
- ⁴¹G. L. Zhao *et al.*, *Phys. Rev. B* **40**, 7999 (1989).
- ⁴²G. L. Zhao and B. N. Harmon, *Phys. Rev. B* **45**, 2818 (1992).
- ⁴³A. Zheludev and S. M. Shapiro, *Solid State Commun.* **98**, 35 (1996).